IEEE Journal of Emerging and Selected Topics in Industrial Electronics, Vol. 2, No. 4, pp 453-463, Oct. 2021.

Lightweight High-Voltage Power Converters for Electro-aerodynamic Propulsion

Yiou He, *Member, IEEE,*, David J. Perreault, *Fellow, IEEE*

***Abstract*—Recent studies in electro-aerodynamic (EAD) propulsion have stimulated the need for lightweight power converters providing outputs at tens of kilovolts and hundreds of watts [2]–[4]. This paper demonstrates a design of a lightweight high-voltage converter operating from a 160 - 225 V dc input and providing dc output of up to 565W at 40 kV. It operates at around 500 kHz and achieves a specific power of 1.15 kW/kg. High voltage converters generally comprise an inverter, a step-up transformer and a rectifier, with the large needed voltage gain distributed among these stages. Several means of realizing these stages are compared in terms of weight. The weight of the converter is minimized by properly selecting and optimizing the design and the voltage gain of each stage within the constraints of device limitations and losses. A prototype circuit is developed based on this approach and used to drive an EAD-propulsion system for an unmanned aerial vehicle (UAV). Moreover, this paper also presents approaches to further improve the specific power of such converters, including better diode utilization and more flexible high voltage transformer design. In addition to addressing the needs for EAD, this research can potentially benefit the development of lightweight high-voltage converters in many other applications where weight and size are important.**

***Index Terms*—High voltage converter, lightweight, Cockcroft-walton, Dickson, high voltage diodes, electro-aerodynamic, EAD**

I. Introduction

High voltage dc-dc power converters are essential in many industrial, medical and aerospace applications [5]–[31]. The specific power, defined as power delivered per unit of weight ($\mathrm{kW\,kg^{-1}}$), of high voltage dc-dc power converters depends strongly on the voltage and power level as well as application requirements. Weight reduction is particularly important for aerospace applications [8]–[13], [23], [24], [27]–[30], therefore has driven research on high voltage dc-dc power converters having high specific power for space and aircraft applications. For megawatt, hundreds-of-kilovolt power converters, specific power can reach as high as $10\,\mathrm{kW/kg}$ [12]. For tens of kV and tens of kW, $1\,\mathrm{kW/kg}$ has been achieved in research papers [12], [31]. However, there has been less research in increasing the specific power of such converters in the sub-kW and medium-to-high tens of kV range.

The paper is an extension of a conference paper, "Y. He, M. Woolston and D. J. Perreault, Design and Implementation of a Lightweight High-Voltage Power Converter for Electro-aerodynamic Propulsion in 2017 IEEE Workshop on Control and Modeling for Power Electronics (COMPEL)" [1]. We extend the work to include more design details and propose improved design approaches.

The authors gratefully acknowledge the support of MIT Lincoln Lab Autonomous Systems Line, the Professor Amar G. Bose Research Grant, and the technical guidance from Mark R. Woolston from MIT Lincoln Lab.

Y. He and D. J. Perreault are with the Dept. of Electrical Engineering and Computer Science, MIT, Cambridge, MA, 02139 (email: djperrea@mit.edu)

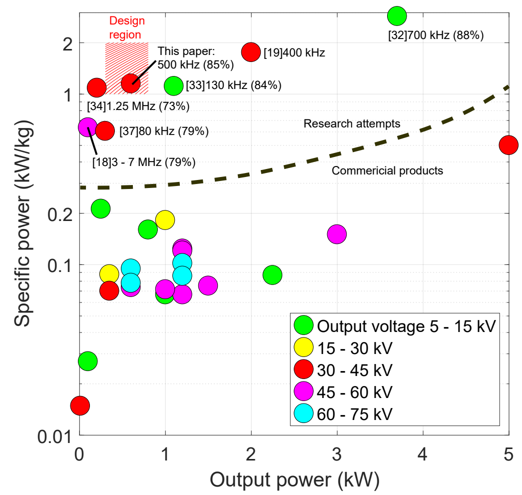

Figure 1: Specific power of commercial high voltage dc-dc converters and academic designs at low to moderate power levels. The reported switching frequencies and efficiencies are listed next to the citations. The design region marks the requirements of interest in this paper.

In Figure 1, a review of commercial products and academic designs in this power and voltage range reveals that the specific power of commercial converters is typically around $0.1\,\mathrm{kW/kg}$. In these converters, the switching frequency typically lies around $100\,\mathrm{kHz}$ or lower, resulting in bulky magnetics and capacitors. There have been research attempts ([18], [19], [32]–[35]) to increase the switching frequency and thus the specific power, but these have largely focused on cases of relatively low output voltage ($\leq 20\,\mathrm{kV}$) [32], [33], [35], and/or out of the power range of interest ($\geq 2\,\mathrm{kW}$ [19], [32] or $\leq 200\,\mathrm{W}$ [18], [34]). See [36] for the detailed list of products and academic papers in this comparison[1].

Aerospace applications requiring low-power, high voltage conversion are emerging in which specific power is a major consideration. For example, electro-aerodynamic (EAD) aircraft propulsion, which uses a set of "solid-state" electrodes to generate ions in air and accelerate the ions to produce a thrust force for propelling aircraft, requires lightweight high voltage power [2], [3], [38], [39]. Most EAD systems use a corona discharge to produce ions, whereby a high potential gradient near a set electrodes with high radius of curvature (e.g. needlepoint electrodes) results in a self-sustaining production of ions, although systems with other ion sources have been demonstrated [40], [41]. In both cases, voltage levels of tens of kilovolts are required to produce useful levels of thrust [2]–[4]. Since EAD propulsion has no moving parts and does

[1]Precise weights of academic designs are not documented in [19], [32], [33], [37] thus the authors estimated these numbers from info in the papers.

not require propellers or turbines to produce thrust, it has the potential to make aircraft quieter, safer, and more robust. In particular, EAD propulsion has shown promise in UAV applications [2]–[4], however, no EAD UAV was ever flown prior to the work by the authors and colleagues [42], in large part due to the weight of the required power electronics. For the EAD propulsion system of interest, the desired voltage and power are identified to be medium-to-high tens of kV and hundreds of watts [2]–[4]. The specific power of the converter needs to be $\geq 1\,\mathrm{kW/kg}$ and still higher is preferable as technology allows.

This paper explores the design of a lightweight high-voltage power converter suitable for EAD propulsion systems. A high voltage converter typically consists of three stages: an inverter stage, an isolation/transformation stage and an ac-dc rectifier stage. The paper firstly compares different approaches and topologies to realize each stage in terms of the resulting weight. Furthermore, the overall weight of a converter based on the best identified approach is optimized by sweeping through combinations of voltage gains for the different stages with considerations of device limitations and losses. The optimized converter design is selected, which consists of three stages: a series–parallel resonant inverter, a high-voltage transformer, and a full-wave Cockcroft–Walton multiplier. The optimized stage contributes nominal voltage gains of about 2.5x, $\sim$15x and $\sim$5.6x respectively for a nominal voltage gain of 210 and a maximum voltage gain of 250. A prototype converter is constructed and tested converting a battery voltage of $160\,\mathrm{V}$ to $225\,\mathrm{V}$ to a $40\,\mathrm{kV}$ output voltage and providing up to $565\,\mathrm{W}$. At the peak output voltage and power, it switches at $\sim 500\,\mathrm{kHz}$, achieves an efficiency of $85\,\%$ and a specific power of $1.15\,\mathrm{kW\,kg^{-1}}$. The prototype was used to enable the first flight of an EAD aeroplane [42]. The paper also explores approaches that may be exploited to achieve even higher specific power of such high-voltage low-power converters.

Section II explores the design goals at a high level, analyzing trade-offs of different approaches and topologies to realize each stage. Narrowing down to the specific design target of the EAD application, Section III selects and optimizes the topology of the converter, taking into consideration the practical constraints of available devices. Section IV describes practical issues in building such a lightweight high voltage dc-dc converter prototype, and presents experimental results of the prototype converter. Section V presents ways to further increase the specific power. Section VI concludes the paper.

II. Topology comparison

High voltage step up dc-dc converters achieve a large step-up voltage ratio using a combination of: (1) resonant and/or multi-level inverters; (2) large-step-up-ratio isolation stage; (3) voltage multiplier rectification stage; and (4) parallel-input series-output structures [43]. This section compares the weight of different topologies/approaches to realize each stage. Section II-A compares the weights of 4 voltage multiplier topologies considering the characteristics of available high voltage capacitors and diodes. Section II-B compares the weight of conventional cored transformers, resonant transformers and piezoelectric transformers. Section II-C briefly analyzes the trade-offs of each resonant inverter topologies.

A. Voltage Multiplier

The achievable weights of voltage multipliers depend substantially on available high voltage capacitors and diodes.

1) High voltage capacitor selection: Mica, film and ceramic capacitors are commonly used in high voltage converters. For high-voltage low-power applications, the rated voltage, the capacitance and the weight of the capacitors are three main considerations. Their ESR and current carrying capability are less important because of the relatively small output current.

Capacitor weight varies widely across rated voltage, capacitance, materials, package, and manufacturer. When the rated voltage is below $\sim 5\,\mathrm{kV}$, there are Surface Mount Technology (SMT) options in all three material classes, among which ceramic capacitors with similar capacitance yield slightly lower weight. When the rated voltage is above $8\,\mathrm{kV}$, there are limited options. Ceramic capacitors with leads offer medium capacitance (up to $1\,\mathrm{nF}$) and relatively high rated voltage (up to $15\,\mathrm{kV}$), and are much lighter options compared with ceramic screw-mount capacitors, Mica and film capacitors.

To realize a capacitor blocking above $8\,\mathrm{kV}$, the two lightest options are 1) using ceramic SMT ones rated below 5kV in series and parallel 2) using a single ceramic through-hole one.

Among the investigated parts, Murata DHR series ceramic through-hole capacitors have the least weight in the $6.3\,\mathrm{kV}$ to $15\,\mathrm{kV}$ range. At a given rated voltage, the weight of the capacitor is shown to be proportional to its capacitance, thus a linear relationship is extrapolated for other capacitances at this voltage rating[2]. See Fig. 2 for examples in the range of $10\,\mathrm{kV}$ to $15\,\mathrm{kV}$ and [36] for more details.

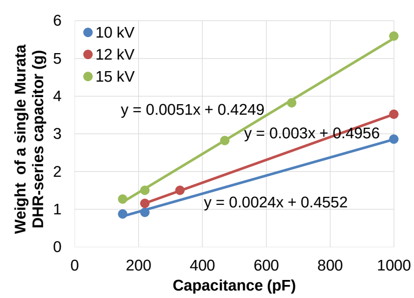

Figure 2: Capacitance and voltage dependency of Murata DHR series HV capacitors (the dots are the measured weights and the lines are linear fits.)

2) High voltage diode selection: High voltage diodes are a key limitation in building a high frequency high voltage converter at tens of kV and hundreds of watts. Traditional silicon high-voltage diodes ($\geq 8\,\mathrm{kV}$) have longer recovery times compared to their low-voltage counterparts, thus are typically used at frequencies below $100\,\mathrm{kHz}$. Commercially available and affordable high voltage SiC schottky diodes are mostly rated under $3.3\,\mathrm{kV}$. They exhibit little recovery time[3]

[2]In the same family from the same manufacturer. Note that the linear fits vary significantly for other manufacturers, series and materials

[3]There is a non-zero “switching time” listed in the datasheet of some of these diodes (for example, the $3.3\,\mathrm{kV}$ SiC schottky diode GAP3SLT33-214).

but large parasitic capacitance since they are mainly designed for high current applications and have a large die size.

Cree's C4D02120A, GeneSiC's GAP3SLT33-214 and VMI's X150FF3 are considered in later studies in Section III because of their small recovery time and relatively low parasitic capacitance. See other device types considered in [36], [44]. There have been also emerging SiC PiN diodes $8\,\mathrm{kV}$ and $15\,\mathrm{kV}$ ones from GeneSiC that could be potential options if cost were not a consideration.

The nominal design frequency is chosen to be $500\,\mathrm{kHz}$ considering steep increases in loss that are observed for many diodes (including the one selected) at higher frequencies.

3) Weight study of various voltage multiplier topologies: The typical topologies of the voltage multipliers used in high voltage converters are shown in Fig. 3. All flying capacitors are odd-indexed and all output capacitors are even-indexed.

We approximate the weight of the voltage multiplier as the sum of the weights of its capacitors. The weights of multipliers in each topology achieving a $40\,\mathrm{kV}$ $700\,\mathrm{W}$ output at different input voltages (thus different gains) are compared in Fig. 4a.

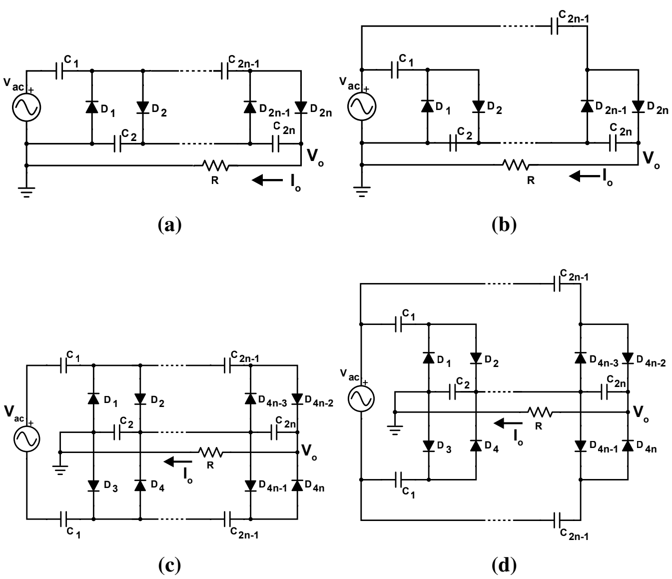

Figure 3: Four basic voltage multiplier topologies (showing single polarity) (a) Half-wave Cockcroft-Walton, (b) Half-wave Dickson, (c) Full-wave Cockcroft-Walton, and (d) Full-wave Dickson.

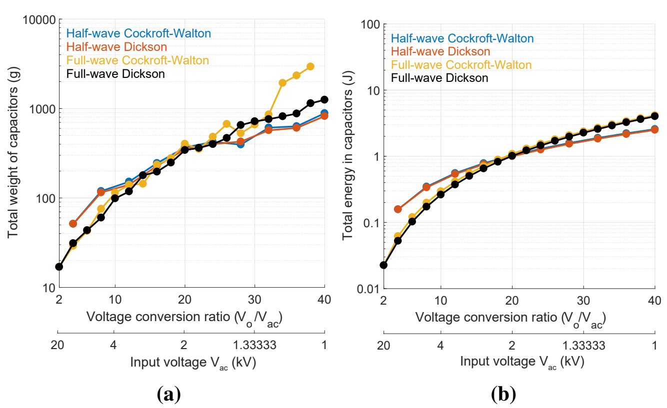

Figure 4: (a) Total weight of the capacitors and (b) total energy stored in the capacitors of the Cockcroft-Walton and Dickson voltage multipliers as a function of converstion ratio (20 kV 350 W output)

At the power and voltage level in this application, and with the device considerations described above, Cockcroft-Walton topologies yield similar weight with Dickson topologies but have easier implementation[4]. When the required voltage gain is lower than 10, full-wave topologies yield lower total weight (owing to interleaving reducing output capacitance), and so are strongly preferred; when the required voltage gain is higher than 25, half-wave topologies yield lower total weight (because they provide the same voltage gain with a halved number of stages, and a further halved flying capacitor count, compared with their full-wave counterparts). This trend coincides with the total energy storied in the capacitors (Fig. 4b). The variations between the weight and the energy can be explained by the discrete nature of the capacitors' energy density.

The process of the weight comparison is illustrated below: we first consider a bi-polar (or interleaved) voltage multipliers with each polarity containing n stages to process half of the desired power and voltage. Then, we pick a topology and calculate the weight of each capacitor. To do so, we identify the voltage across each capacitor, and calculate their capacitances following two specifications below. An assumptions is made to simplify the calculation: in a given topology, all flying capacitors (odd-indexed) are the same and all output capacitors (even-indexed) are the same. For example, in a half-wave Cockcroft-walton voltage multiplier, $C_1 = C_3 = ... = C_{2n-1} \triangleq C_{odd}$, $C_2 = C_4 = ... = C_{2n} \triangleq C_{even}$.

- The even-indexed capacitors in half-wave topologies are sized such that the voltage ripple is less than $100\,\mathrm{V}$ (see [36] for the voltage ripple as a function of even-indexed capacitances). Ideally for full-wave topologies, the ripples of the two half-wave would cancel each other and no output capacitors are needed. However, to account for non-idealities, we size these even-indexed capacitors such that the RC time constant of the effective total output capacitance and the load is 20 times the switching period.
- The odd-indexed capacitors in all topologies are then sized such that the voltage droop due to the capacitor charge loss [45] is less than $2.5\,\%$ of $20\,\mathrm{kV}$ ($5\,\%$ for the full converter outputting $40\,\mathrm{kV}$). See [36] for the voltage droops as functions of capacitances.

Then, for each capacitor, we calculate its weight following the linear relationships with two assumptions: 1) the rated voltage of the capacitor is twice its required blocking voltage. 2) allow up to 4 discrete capacitors to connect in series and 20 in parallel to achieve the desired blocking voltage and capacitance. Lastly, we sum up the capacitor weight and double it (due to the bi-polar design) to obtain the "total weight" of the voltage multiplier. The total energy stored in capacitors is calculated in the same fashion.

B. Isolation Stage

Three isolation methods are compared in terms of weight: full-core transformers, air-core resonant transformers and piezoelectric transformers.

[4]In Cockcroft-Walton topologies, capacitors and diodes block the same voltage other than the flying capacitor in the 1st stage. Whereas in Dickson topologies, the blocking voltage increases in higher stages.

Full-core transformers dominate the isolation stage design in traditional high-voltage converters. A study in [12] for high-power low-frequency transformers ($0.1\,\mathrm{MW}$ to $100\,\mathrm{MW}$, tens of kHz, no voltage insulation requirements were considered) shows the theoretical specific power of transformers roughly scales with its frequency f and power P as $f^{0.75}P^{0.25}$, indicating that specific power improves with higher power. Air-core resonant transformers (e.g., Tesla coil) eliminate the use of a heavy core and could potentially be light. However, it is a highly tuned structure, sensitive to parasitic inductance and capacitance, and may be relatively large in size [46], [47]. Piezoelectric transformers can achieve a power density of $40\,\mathrm{W/cm^3}$ [48], especially suitable for high voltage low power (e.g., tens of watts) applications. They have been used in space applications at below $20\,\mathrm{kV}$ and $200\,\mathrm{W}$ [49]. However when scaling up in power, one needs to connect existing piezoelectric transformers in series and in parallel and the advantage in power density are less obvious.

To illustrate these tradeoffs, isolation stages were designed and the resulting weights were compared, as shown in Table. I. Full-core and air-core transformer were both designed to step up a $500\,\mathrm{V}$ amplitude $500\,\mathrm{kHz}$ ac to a $10\,\mathrm{kV}$ amplitude ac, delivering $1\,\mathrm{kW}$. See detailed designs in [36].

Table I: Weight comparison of different isolation stages.
† Bounds correspond to different insulation materials. Lower bound is Nylon 6/6 (glass) and upper bound is PTFE (glass).
‡ Bounds correspond to whether to include a supportive structure for the secondary winding made with a $0.1\,\mathrm{mm}$ thick Nylon 6/6 tube.
†† The unit weight is estimated with the same density as [50] and a size of $120 \times 8 \times 5.7\mathrm{mm}$. Assume 7 in series 17 in parallel.

Type	Rated power	Rated voltage	Total weight	Specific power
Ferrite core transformer	$1\,\mathrm{kW}$	$10\,\mathrm{kV}$	250 - 320g †	3.1 - 4kW kg^{-1}
Tesla coil	$1\,\mathrm{kW}$	$10\,\mathrm{kV}$	135 - 152g ‡	6.6 - 7.4kW kg^{-1}
Piezoelectric transformer	Use STEMiNC SMMTF53P2S40 2W 1.2 kV piece, 9S60P [50]		1080	0.93
	Use Face Transornor 1.5 kV piece, 7S17P [51]		1095 † †	0.92

The full-core transformer design yields a specific power of 3.1 to $4\,\mathrm{kW\,kg^{-1}}$. The choice of the insulation material around the secondary wire and the core affects the total weight and the winding's parasitic capacitance. Here we give a lower bound of $250\,\mathrm{g}$ where glass-filled Nylon 6/6 is used and an upper bound of $320\,\mathrm{g}$ where glass-filled PTFE is used.

The air-core resonant transformer, designed following [46], [47], yields $135\,\mathrm{g}$ and can reach $152\,\mathrm{g}$ and higher with additional supportive structure. The air-core resonant transformer shows doubled specific power compared with the full-core transformer, but is less efficient. This would require heavier energy source (e.g., battery) in the intended EAD application. In addition, it is necessarily large in size, less robust in construction and requires narrow-band operation, which makes this option less appealing.

Piezoelectric transformers are designed to provide the same output voltage, $10\,\mathrm{kV}$ in amplitude, and output power, $1\,\mathrm{kW}$, by connecting existing piezoelectric transformers from Transonor [51] and STEMiNC [50] in series and in parallel. We leave the input voltage parameter uncontrolled. As an example, we use SMMTF53P2S40 (rated for $2\,\mathrm{W}$ $1.2\,\mathrm{kV}$ output): the weight and the dimension of a single off-the-shelf part are $2\,\mathrm{g}$ and $35.8 \times 8.8 \times 3.8\mathrm{mm}$, thus its density is $1.67\,\mathrm{g\,cm^{-3}}$. To achieve $10\,\mathrm{kV}$ and $1\,\mathrm{kW}$, we need 9 modules in series and 60 in parallel, yielding $1080\,\mathrm{g}$ and $0.93\,\mathrm{kW\,kg^{-1}}$.

Considering both feasibility and achievable specific power, full-core transformers are compact, robust, and more flexible in use than air-core resonant transformers or piezoelectric transformers at the voltage and power level, so are preferred.

C. Resonant topology selection

High voltage transformers have a large number of secondary turns, resulting in large parasitic capacitances. To usefully incorporate this capacitance into circuit operation, a parallel resonant inverter or a series-parallel resonant inverter is suitable. A full-bridge series-parallel resonant inverter is chosen because: 1) it provides a factor of 2 in the voltage gain with negligible weight gain; 2) it shows high efficiency in both light load and heavy load; 3) it has a series capacitor to block dc voltage and thus prevent transformer saturation [52], [53].

III. Design Optimization

Based on the weight study and engineering considerations such as risks and practicality, a cored-transformer and a series-parallel resonant inverter are chosen. Different distributions of voltage gains among the three stages can result in different overall weights. Section III-A explains that in our design, the available diodes set the transformer secondary voltage, which decouple the voltage multiplier stage from the overall optimization. Section III-B comprehensively designs the inverter and transformer stages to minimize the total weight of the passives while maintaining a good efficiency.

A. Finalizing the voltage multiplier

In practice, the transformer parasitic capacitance and the junction capacitance of the diodes are reflected to the transformer primary with a multiple of the square of the turns ratio. Too much these capacitance can result in large circulating current in the resonant tank and thus lower efficiency.

Using Cree's C4D02120A, GeneSiC's GAP3SLT33-214 and VMI's X150FF3 respectively, a single-stage full-wave Cockcroft-walton voltage multiplier is simulated in LTspice (Fig. 5a). Each voltage multiplier is driven by a $500\,\mathrm{kHz}$ $0.5\,\mathrm{A}$ current source and uses the same transformer. The diode in the voltage multiplier consists of either one $15\,\mathrm{kV}$ X150FF3, or 13 $1.2\,\mathrm{kV}$ C4D02120A or 5 $3.3\,\mathrm{kV}$ GAP3SLT33, yielding a diode blocking voltage of $\sim 15\,\mathrm{kV}$. As a reference, a voltage multiplier with ideal $15\,\mathrm{kV}$ diodes that have no forward voltage drop or parasitic capacitance is also simulated.

The simulation results in Fig. 5 show that the voltage droop, defined as the difference between the output voltage when using ideal diodes and those when using investigated diodes, is the lowest with X150FF3 diodes. Using multiple SiC diodes theoretically reduces the overall parasitic capacitance, but since their junction capacitance is much larger than that of X150FF3, the simulation still shows unacceptably large droop. In addition, series-connecting multiple SiC diodes can

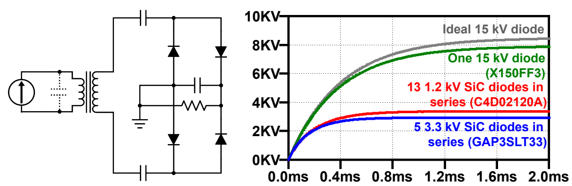

(a) (b)

Figure 5: (a) Simulation schematics and (b) the output voltage of three single-stage full-wave cockcroft-walton multipliers using three different diodes. In the schematic, the dashed-line capacitor represents the parasitic capacitance reflected to the transformer primary.

potentially require balance circuits and add more complexity. Therefore, in this design, the X150FF3 is selected as the most effective available diode. To simplify the design and because of second-order effects that can occur [44], we do not consider connecting multiple of X150FF3 in series as an equivalent higher voltage diode, which sets the output of the transformer to be less than ~7.5 kV (considering a 50% voltage derating).

Referring back to the voltage multiplier weight study in Fig. 4a, a 3-stage bipolar (6-stage total) full-wave Cockcroft-Walton voltage multiplier can convert 7.5 kV to 40 kV and yield a light weight. Compared to a 3-stage full-wave Dickson, the Cockroft-Walton voltage multiplier has a simpler implementation because most flying capacitors have the same capacitances and block the same voltages thus is chosen.

B. Weight study of the inverter and the transformer

The series-parallel inverter and the transformer stages (Fig. 6) are required to convert $V_{DC} = 200\,\text{V}$ dc to $V_{Sec} = 7.5\,\text{kV}$ ac at 500 kHz. The transformer is chosen to be center-tapped so that it handles a bi-polar output voltage rather than a unipolar output voltage, which reduces the isolation voltage requirement by half. To account for the losses in the voltage multiplier, we design at $P_{Sec} = 750\,\text{W}$ rather than 700 W. To simplify the weight analysis, we use the Fundamental Harmonic Approximation [52] method to analyze the inverter operation and assume V_{Pri} to be sinusoidal.

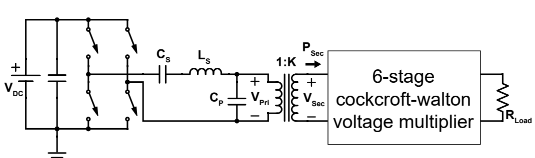

Figure 6: The inverter and the transformer stages. The resonant tank input is a square wave of amplitude V_{DC} containing no dc component.

The weight of the two stages is dominated by magnetics (the inductor and the transformer), thus the design space is explored to minimize the summed weight while maintaining good efficiency[5]. The optimization process contains five steps:

- Select a set of operating variables: the resonant tank quality factor Q, the tank natural frequency f_0, the series and parallel resonant capacitance ratio $A = C_P/C_S$, and the transformer voltage step up ratio K (i.e. turns ratio). Then the inductance and capacitances of the resonant tank (L_S, C_S, C_P), the tank voltage gain $G = V_{Pri}/V_{DC}$ and the tank current $I_{L_{max}}$ can be calculated (see [36] for details). We keep the sets that yield a transformer output voltage $V_{Sec} = V_{DC} \times G \times K \in [7.5kV, 9kV]$.
- Design the lightest transformer that satisfies an input voltage of $V_{DC} \times G$, turns ratio K, output power P_{Sec} = 750 W and a set of constraints on efficiency, temperature and packing factor. See detailed methods in [36].
- Design the lightest inductor with inductance L_S, maximum current $I_{L_{max}}$ and a set of constraints on efficiency, temperature and packing factor. See details in [36].
- Sweep all sets of operating variables and find the lightest summed weight of the inductor and the transformer. The design space we explored is: $0.2 \le Q \le 10$, $0.1 \le A \le 10$, $450\,\text{kHz} \le f_0 \le 500\,\text{kHz}$, $5 \le K \le 30$.
- Refine the lightest designs by checking the parasitics of the transformer: 1) if the transformer leakage inductance is not negligible compared with L_s, then redesign the inductor. 2) if the transformer parasitic capacitance is larger than C_P, then sectioning its secondary winding.

To simplify the study of this prototype, we consider: 1) center-leg winding on E-type cores for both the transformer and the inductor to ensure good coupling[6]; 2) only off-the-shelf core sizes. Customized cores may yield more optimal designs and will be discussed in Section V; 3) the secondary wire fixed as Teledyne Reynolds AWG28 18 kV FEP wire[7].

C. Optimal weight and voltage gain distribution

In Fig. 7, we plot the lightest overall weights of magnetic components and their corresponding inductor and transformer weights against the transformer primary voltages V_{Pri} in the range of 200 V to 1800 V, which is a function of Q, A, f_0, K. The lightest overall weight shows a clearer trend with V_{Pri} than any of Q, A, f_0, K, thus is plotted.

Figure 7a suggests the overall weight of magnetic components first decreases and then increases with V_{Pri}. It reaches the lowest when V_{Pri} is around 400 V to 600 V. For this range of V_{pri}, the resonant tank provides a gain of $G \sim 2-3\times$ and the transformer provides a gain of $K \sim 18-12\times$. A valley point is reached because of how the core sizes required for the inductor and transformer trade with the voltage gains provided:

- The transformer weight (Fig. 7b) first decreases then increases with V_{Pri}. All designs are temperature limited.
  - When $V_{pri} \le$400 V, a larger turns ratio of the transformer requires a larger amount of windings and a bigger core for the windings, yielding a heavier weight.
  - When V_{pri} is in 400 V – 1.5 kV, the volt-second on the core keeps increasing, but the transformer weight stays relatively flat because 1) to keep the maximum flux density B_m low, we need a higher primary number of turns N_p. But higher V_{pri} results in lower turns ratios, yielding unchanged (or even reduced) number of secondary turns, thus the copper volume and weight

[5]The transformer is to be ≥95 % efficient and the inductor is to be ≥98 %

[6]This makes the transformer leakage inductance small compared with L_s

[7]P/N 178-5790, this is the smallest gauge high voltage wire (≥15 kV) we found in a time limited search. Its voltage rating and gauge size may be conservative but provide good design margin

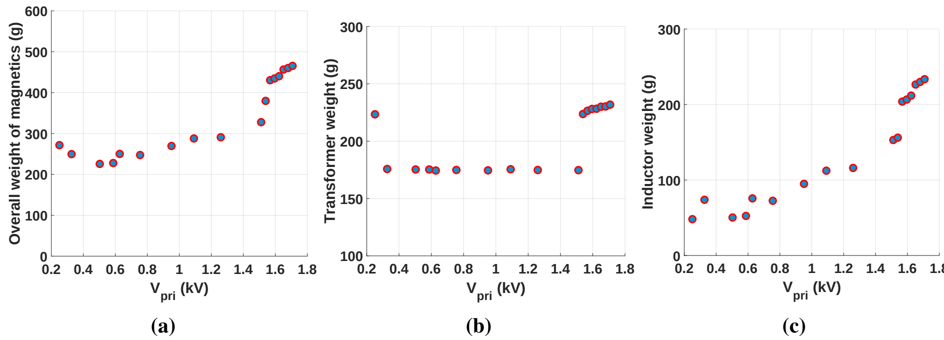

Figure 7: Lightest overall weights of (a) both the inductor and the transformer, (b) the corresponding inductor weights and (c) the corresponding transformer weights against the transformer primary voltages V_{Pri}. The discreteness is due to our assumptions to use discrete off-the-shelf core shapes, wires and discrete operating variables Q, A, f_0, K. Customized cores and wires can yield to a lighter overall weight, as will be discussed in Section V-B.

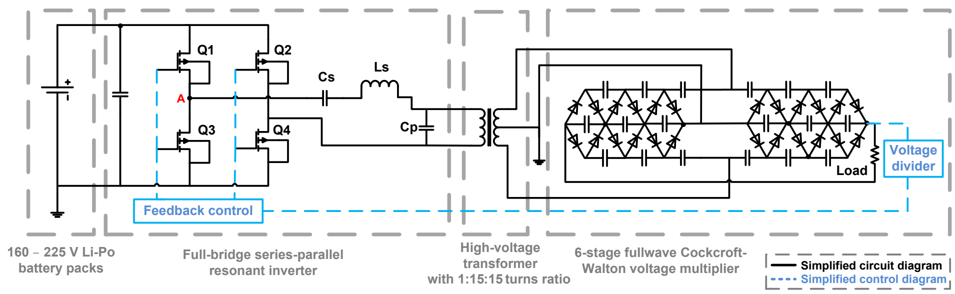

Figure 8: Final design of the developed high voltage dc-dc converter. Node A marked in red corresponds to the switching node waveform in Fig. 10.

stay relatively flat; 2) the core volume and weight also remain unchanged because no bigger cross-sectional area is needed to balance the increasing volt-second, and similar cores can be used to fit the relatively unchanged winding volume.

– When V_{pri} $\geq$1.5 kV, the volt-seconds keeps increasing, the original core height is not enough to fit the increasing amount of primary number of turns N_p, thus a larger core with bigger window height is needed, yielding a heavier weight.

- The inductor weight (Fig. 7c) increases with V_{Pri}, especially when $V_{pri} \geq 0.8\,\mathrm{kV}$ (corresponding to the tank voltage gain $G \geq\sim 5$ and tank quality factor $Q \geq\sim 3$). All designs are also temperature limited. At higher tank gain G, to keep the maximum flux density low, more turns and bigger core cross-sectional area are required, yielding to heavier core and copper weights.

For the final design, we pick V_{Pri} to be at $\sim$500 V, the resonant tank Q is ~ 2, the tank voltage gain $G \sim 2.5$ and the transformer turns ratio is $K = 15$. The final converter topology is shown in Fig. 8. It comprises a series-parallel resonant inverter, a 1:15:15 ferrite-cored high voltage transformer and a 6-stage bi-polar full-wave Cockcroft-Walton multiplier.

D. Sectioning the transformer secondary winding

When designing the transformer, an important criterion is to use its parasitic capacitance as part of the parallel resonant capacitance C_p. A multi-section secondary is a common solution to reduce the self-capacitance of the winding. A rule of thumb is that with n-sections, the self-capacitance can be reduced to $1/n$ [54]. The winding-to-core capacitance is considered to be not affected by any sectioning. See [36] for detailed equations.

In this study, we consider one multi-section secondary and the section number is swept between 1 and 4. In the final design, the transformer secondary is sectioned into 2 sections. No higher number of sections is needed.

IV. Experimental results

A prototype converter with closed-loop voltage feedback control based on the optimized design in Fig. 8 was built, as shown in Fig. 9. All the sensing, control and driver circuits are integrated on the printed circuit board and it needs no additional components other than a logic power supplied by a 3.7 V LiPO battery for the EAD flight demonstrations. There have also been special considerations in construction of the voltage multiplier (include heatsink design, FEA thermal and field analysis). See [36] for details. We also explicitly used air isolation as a strategy which improves the specific power at the expense of the power density.

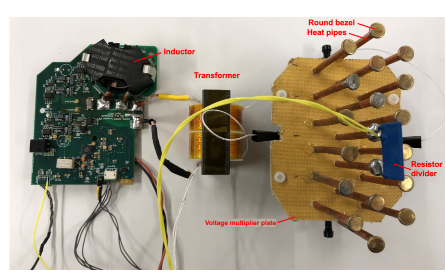

Figure 9: 200 V to 40 kV high voltage dc-dc converter prototype

Fig. 10 shows the waveforms of the converter running at 500 kHz and converting 177 V to 38 kV at $\sim$480 W. The

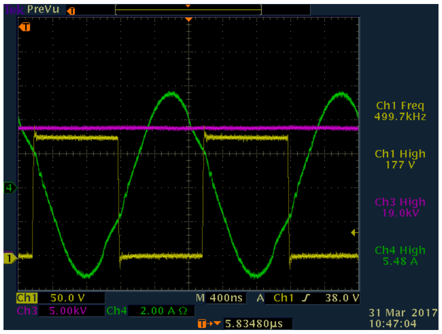

Figure 10: Experimental waveforms of the developed high voltage dc-dc converter prototype outputting $\sim$480 W 38 kV (Ch1 (yellow): half-bridge switching node voltage (Node A marked in red in Fig. 8); Ch3 (pink): half of the output voltage; Ch4 (green): resonant tank current)

converter achieves an efficiency of 83 % at 480 W 38 kV and 82 % at 300 W 40.4 kV. We were not able to push to above 550 W output before the MOSFETs GS66504B overheated. A previous version of the inverter using EPC 2025 MOSFETs were tested at 565 W 39 kV output, achieving 85% efficiency. EPC 2025 went obsolete therefore we switched to GS66504B. The largest component of loss is estimated to result from the high voltage diodes, followed by the transformer, with MOSFETs and inductor losses being smaller. The diode loss was moreover the dominant limitation preventing increases in frequency and specific power in this design, resulting in the diode investigation in [44].

The prototype was used to drive electrode thrusters of an EAD aeroplane and demonstrated the first flight of such an airplane [42]. The finalized components in the converter and the weight breakdown are listed in Table II. The prototype achieves a specific power of $1.15\,\mathrm{kW\,kg^{-1}}$ (565 W/491 g) and a box power density of $0.56\,\mathrm{W\,cm^{-3}}$ (565 W/1007 $\mathrm{cm^3}$). In this design, the specific power is a more important metric given the main goal is to reduce the weight rather than the volume of the converter.

V. Paths to further improve the specific power

In exploring future designs of EADs, we identify two new requirements for the high voltage converter:

- Higher output voltage at 40 kV to 60 kV or even higher with 1) similar input voltage, 2) similar output power of up to 600 W, and 3) similar (85%) or higher efficiency
- Higher specific power at or above $1.5\,\mathrm{kW\,kg^{-1}}$.

We present two ways to further improve the specific power of a converter that can convert 200 V to 60 kV at 600 W:

- In Section V-A, we incorporate insights learned about high voltage diodes in [44] in the design. This allows us to: 1) remove cooling fixtures and their associated weights; 2) increase the switching frequency to $\geq$1 MHz, which further reduces the size and weight of passives.
- In Section V-B, we explore more flexible high voltage transformer designs that may yield lower weight, including customized core size and core shape, different winding patterns, and various high voltage wires.

A. Improved voltage multiplier design

One of the bottlenecks to achieving high frequency at high output voltage while preserving high efficiency is the lack of low-loss high-frequency high-voltage diodes [55]. In [44], we tested 37 off-the-shelf diodes in a full-bridge rectifier switching at both 600 kHz and 1 MHz, and each diode blocking 50 % of their rated voltage and carrying an average current 5 % to 10 % of their rated dc current (we call these "single diode tests"). We identified 17 diodes with a maximum temperature rise lower than 100 °C at both frequencies. These diodes are promising candidates for the improved voltage multiplier.

We want to narrow down the selections to the diodes that are both lighter weight and less lossy. We use the temperature rises of each diode at 600 kHz and 1 MHz in the single diode tests as their loss metrics. We define a weight metric for each diode as the unit weight of the diode multiplied by the number of diodes needed in series to block a dc voltage V (with a 50% derating on the rated voltage) then the number of diodes needed in parallel to carry a dc current I (with a 10% derating on the rated average forward current). We pick $V = 60\,\mathrm{kV}$ and $I = 20\,\mathrm{mA}$ to represent high-voltage low-current applications.

Figure 11a and Fig. 11b plot the defined weight metric against the defined loss metric at 600 kHz and 1 MHz respectively. Each data point is labeled with the diode index. Diode No. 18 (X150FF3) is used in the 1st-generation high voltage dc-dc converter. Details of these diodes are listed in Table III.

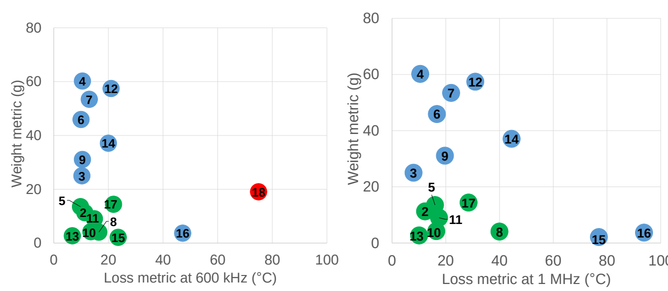

(a) (b)

Figure 11: The defined weight metric of each diode plotted against the defined loss metric at a) 600 kHz and b) 1 MHz for realizing an effective rectifier device for use at 60 kV and 20 mA. The ones in green are promising. Diode No. 18 is used in 1st-generation converter.

We prefer diodes with a temperature rise $\leq$ 40 °C and a weight metric $\leq$ 20 g at both frequencies (highlighted in green). We pick 40 °C because 1) this temperature rise is likely a conservative estimate of the actual temperature rise of the diodes when connected in series and/or used in a multi-stage voltage multiplier; 2) when it is above 40 °C, a heat sink is likely required. We pick 20 g because there seems a clear separation between 20 g and the next lightest.

In addition, in [44] we also tested these diodes in the same full-bridge rectifier, but with each rectifier leg consisting of several diodes connected in series. Higher temperature rises are observed due to the imbalance in voltage distribution among the series-connected diodes. Diodes No. 10 and 13 exhibit much severer temperature and voltage imbalance when connected in series, thus are removed.

We narrow down to 5 diodes (No. 2, 5, 8, 11, 17) as candidates. With the identified diodes and following similar

Table II: Specifications and component weight breakdown of the prototype high voltage power converter. The total weight here does not include that of the supportive structures and the peripheral circuits which are necessary for the flight. (‡ The same core in TDK N49 would yield to slightly lower loss but not available; † The primary turns is reduced to 10 and the secondary correspondingly to 150 (1:15), compared with the designed 13 and 196 (1:15) due to imperfection in hand-winding and added insulation thickness in the practical construction.)

Stage	Component	Manufacturer and Part Number	Value/Description	Weight	Weight %
Inverter	MOSFETs	GaN system GS66504B	-	56 g	11.4%
	C_s	TDK C3216C0G Series	19.6 nF		
	C_p	Parasitic capacitance	∼5 nF		
	Inductor L_s†	RM14I core in TDK N49; MWS wire AWG14(150/36)	11 turns, air gap 0.87 mm, 33.2 µH	80 g	16.3%
Trans-former	Core ‡	ETD49/25/16, Ferroxcube 3F35		124 g	In total, 170 g. 34.6%
	Primary†	MWS AWG 16 (350/42)	10 turns, 1 layer; Total length 0.52 m; Unit weight 18.45 g m^{-1}	9.6 g	
	Secondary†	Teledyne Reynolds AWG28 18kV FEP wire (P/N 178-5790)	150 turns, 2 section. In each section, 5 layer 15 turns per layer; Total length 12.5 m; Unit weight 2.68 g m^{-1}.	34 g	
	Bobbin	ABS 3D printed	-	2.4 g	
Voltage Multi-plier	C_{odd}	Murata DHR4E4B102K2BB	1 nF. Unit weight 3.3 g. Qty. 12.	40 g	In total, 115.3 g 23.5%
	C_{even}	Murata DHR4E4B681K2BB	0.68 nF. Unit weight 2.3 g. Qty. 6.	14 g	
	Diodes	VMI X150FF3	Unit weight 0.51 g. Qty. 48.	25 g	
	Bezel joints	Metalliferous BR8818	Unit weight 0.8 g with solders. Qty. 19.	31 g	
	Divider	OHMITE SM204RD-0009	100M/100k 1000:1 resistor, 1%	1.7 g	
	Connectors	Pomona Electronics 5936-0 and 5935-0	Unit weight 0.6 g. Qty. 6.	3.6 g	
	Output wire	Teledyne Reynolds AWG22 30kV Silicone coated FEP wire (P/N 178-8781)		-	-
Heat sink	Heat pipes	Wakefield-Vette 121686_R EV1. 7mm long 4mm OD.	Unit weight 3.6 g. Qty. 19.	69 g	14%
Total weight				491 g	100%

Diode index	Manufacturer	Part Number	Rated voltage (V)	Rated current (mA)	Type	Unit weight (g)	Length (mm)	Width (mm)	Temperature rise of one diode (°C)		Loss of one diode at 1 MHz (W)	Test current at 1M (mA)	Forward drop (V)	Capacitance at 0V (pF)
									600 kHz	1 MHz				
1	Wolfspeed	CSD01060E	600	1000	SiC Schottky	0.315	6.73	10.00	9.40	8.40	0.07			
2	Infineon	C3D1P7060Q	600	1700		0.033	3.30	3.30	11.40	12.30	0.08	200.00	2.4	82.5
3	GeneSiC	GB01SLT06	650	1000		0.088	5.59	3.94	10.3	8	0.06			
4	Infineon	IDL02G65C5	650	2000		0.184	8.10	8.10	10.5	10.5	0.09			
5	GeneSiC	GB01SLT12	1200	1000		0.088	5.60	3.95	9.8	16	0.12	200.00	2.4	71.0
6	Infineon	IDM02G120C5	1200	2000		0.315	6.73	10.00	10	16.7	0.13			
7	ST	STPSC5H12B	1200	5000		0.390	6.73	10.00	13	22	0.22			
8	GeneSiC	GAP3SLT33-214	3300	300		0.065	5.59	3.94	16.5	40	0.39	30.00	5.2	38.0
9	Bourns Inc.	CD214A-F1400	400	1000	Si	0.068	5.59	2.92	10.5	19.7	0.18			
10	Taiwan	ESH1GM	400	1000		0.006	2.70	1.35	13.6	16.5	0.10			
11	Taiwan	UF1GLW	400	1000		0.014	3.80	1.90	14.9	17.5	0.19	200.00	1.3	25.0
12	VISHAY	BYV26B	400	1000		0.161	4.00	3.60	21	31	0.31			
13	ROHM	RFU02VSM6S	600	200		0.006	2.50	1.40	6.8	10.1	0.06			
14	VISHAY	BYV26C	600	1000		0.155	4.00	3.60	20	44.5	0.56			
15	ROHM	RFU02VSM8S	800	200		0.007	2.50	1.40	23.6	77	0.32			
16	Dean	SP5LFG	5000	270		0.102	8.55	2.79	47.2	93.8	0.53			
17	Dean	HVEF8P	8000	30		0.082	10.20	2.50	21.9	28.5	0.19	6.00	20.0	0.3
18	VMI	X150FF3	15000	50		0.510	9.14	4.32	75	------------------				

Table III: Specifications of candidate diodes in the 2nd-gen voltage multiplier design. The ones highlighted in red are the most promising. Temperature data, loss data and the manufacturer abbreviation are all the same as in [44].

design methods in Section II, we built weight models for various voltage multipliers which were feed into the overall weight model of the dc-dc converter. See details in [36].

B. Updates on high-voltage transformers

We identify two factors affecting the achievable weight and specific power of a high-voltage transformer: available high-voltage wires and core sizes. Core shapes and winding pattern show some, but not significant, effects on the achievable weight. See detailed analysis in [36].

1) High voltage wires: are offered at limited sizes and voltage ratings, which restricts the design of a high-frequency high-voltage transformer. We survey 190 high voltage wires (both single conductor wires and litz wires) from Teledyne Reynolds and Rubadue rated between 1 kV to 40 kV. For litz wire, we refer the "wire size" as the equivalent size of the litz bundle, and "the single-strand conductor size" as the litz wire size; for single-conductor high voltage wires, we refer both terms as the size of the conductor.

Wire size: We find that the smallest off-the-shelf wire size increases with the wire rated voltage. Between 1 kV to 3 kV, the smallest wire is AWG 40; between 3 kV to 25 kV, it is around AWG 28; above 25 kV, it is AWG 20. There is no available off-the-shelf wire at ≥40 kV. The average current carrying capability of AWG 40, AWG 28 and AWG 20 wires are 25 mA, 0.6 A and 3.9 A respectively at an average current density of 500 A cm^{-2}, a rule-of-thumb for designing transformers with reasonable copper losses. For an example high voltage low power transformer, e.g. outputting 10 kV and 500 W, using wires rated ≥ 10 kV (preferred for insulation purposes) would result in inefficient use of the wire; if we use wires rated at lower voltages, we can fully utilize the copper area, but face increased risk of arcing and engineering complexity (such as sectioning the windings).

Single strand conductor size: Similarly, we find smallest single strand conductor sizes of high voltage wires also increase with the rated voltage. For high-frequency designs, it is preferred to use a single strand conductor size at or smaller than the skin depth [56] because larger sizes increase copper losses owing to proximity effect, take up more window area and add to the total weight. The higher the frequencies and the voltage, the fewer the wire options, thus more limitations on the designs of such a transformer.

Insulation jacket: We find that the insulation thicknesses, though generally increasing with voltage, vary even for wires rated at the same dc voltage from the same manufacturer. For example, 18 kV wires have an insulation thickness range between 0.3 mm to 0.65 mm, corresponding to an effective dielectric strength between 30 kV mm^{-1} to 60 kV mm^{-1}.

In the 1st-generation transformer, the insulation of the secondary wire accounts for ∼15% of the transformer weight. Thus thinner jacket thickness is preferred.

Effects on the weight

All three limitations mentioned above are mismatched across available wires. For example, the wire with the smallest wire size does not have the smallest litz size or the thinnest jacket thickness in. Therefore, the compounded inefficiencies of three factors may result in additional weight, and designing a high-voltage transformer with the most appropriate off-the-shelf wire or with customized wires (if possible) is preferred.

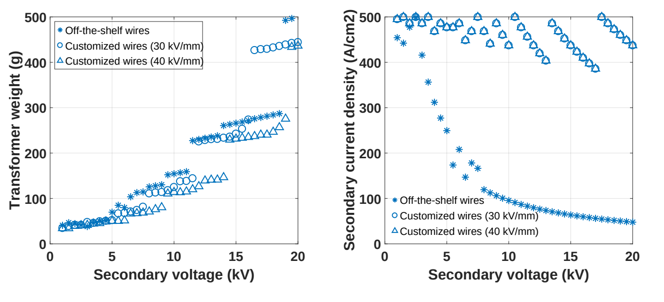

(a) **(b)**

Figure 12: (a) Weight and (b) secondary peak current density of high voltage transformers designed with off-the-shelf wires or customized wires.

.

Figure 12a shows transformer weights and Fig. 12b shows average current density of secondary wires (assuming uniform distribution and ignoring skin or proximity effect) when a transformer is designed using off-the-shelf wires or customized wires with two effective dielectric strengths ($30\,\mathrm{kV\,mm^{-1}}$ and $40\,\mathrm{kV\,mm^{-1}}$). We design the transformer to convert $500\,\mathrm{V}$ to $1\,\mathrm{kV}$ to $20\,\mathrm{kV}$ at $1\,\mathrm{MHz}$ and output $600\,\mathrm{W}$. Four assumptions made across designs are: 1) consider only Ferroxcube off-the-shelf core sizes; 2). use Ferroxcube 3F46 as the core material; 3) secondary wires are rated at 6 times the layer-to-layer secondary voltages; 4) for customized wires, use AWG48 as both the minimal litz size and the minimal wire size.

We conclude from these results that when the secondary voltage is below $5\,\mathrm{kV}$ in amplitude, the weights are not significantly different by using either wire. As the secondary voltage increases, the transformer weight increases discretely – this is a compounded effect of both the wires and the core sizes. Comparing across different types of wires, off-the-shelf wires are used at a much lower current density, taking up the winding space, driving up the core sizes and yielding heavier designs compared to the customized wires.

2) Core sizes, shapes and winding patterns: Manufacturers offer limited and discrete core sizes which fit general designs but may not be optimized for high voltage designs.

EE (Fig. 13a) and ER cores (Fig. 13b) with customizable sizes are considered in the study. EE cores are easy to machine and customize; ER cores are favorable for high voltage designs because they have fewer sharp corners. For both core shapes, we assume that each side leg has half the cross sectional area of the center leg. For ER cores, we also compare center-leg winding and double-leg winding (Fig. 13c).

Figure 14a compares transformer weight when designed using off-the-shelf cores or customized cores. We hold the same design specifications and the assumptions as the study above. To separate the effect of the wires, we consider using customized wires with an effective dielectric strength of

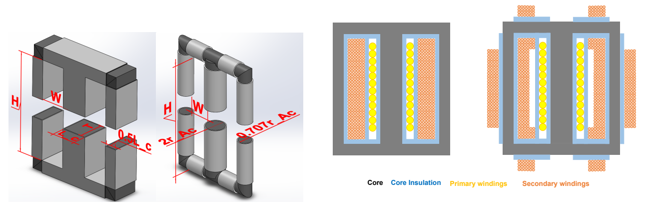

(a) **(b)** **(c)**

Figure 13: (a) EE cores and (b) ER cores (c) front-view of center-leg (left) and double-leg (right) winding considered in the weight study.

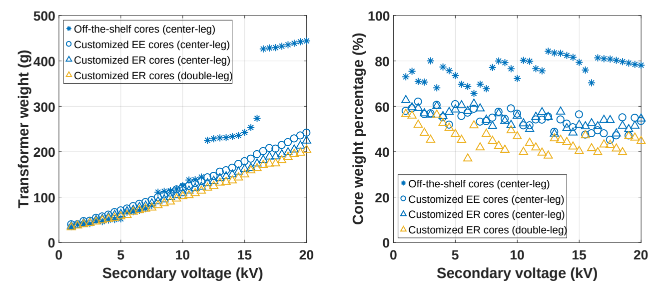

(a) **(b)**

Figure 14: (a) Transformer weight and (b) percentage of core weight in the transforer weight when designing high voltage transformers with off-the-shelf cores or customized EE/ER cores.

$30\,\mathrm{kV\,mm^{-1}}$ across all designs (thus the data with asterisks in Fig. 14 corresponds to the data with circles in Fig. 12).

As the secondary voltage increases (especially above $\sim$$10\,\mathrm{kV}$), customized core sizes become more beneficial as there are fewer and more sparse off-the-shelf core sizes. Among the customized designs, as the voltage increases, the copper and the insulation takes up more of the transformer weight, the core weight percentage reduces from 60% to 50% as the voltages increases from 0-5 kV to 15-20 kV (Fig. 14b).

Figure 14 also suggests different core shapes and different winding patterns have some but not significant influence on the achievable transformer weight. With customization, a transformer weighing $10\,\mathrm{g\,kV^{-1}}$ appears possible when stepping up a $500\,\mathrm{V}$ in amplitude $1\,\mathrm{MHz}$ ac to $5\,\mathrm{kV}$ to $20\,\mathrm{kV}$ at $600\,\mathrm{W}$.

Furthermore, we can incorporate the improved weight study of voltage multipliers and high voltage transformers to comprehensively design the three stages of the high voltage dc-dc converter. The optimization methods are similar with that in Section III-C. With the improved approaches, higher specific power of the high voltage dc-dc converter can be achieved [36].

VI. Conclusion

This paper explores the design space and presents the design of a lightweight high-voltage converter for EAD propulsion applications. Various converter topologies are compared in terms of weight with considerations of device limitations. The weight of the converter is then minimized by design of the voltage gain of each stage. A prototype converter rated at 40 kV and 565 W is built, tested and achieves a specific power of 1.15 kW/kg, above other designs in its power and voltage class. Furthermore, several approaches to further improve the specific power of such a converter are presented. These design approaches can likewise be used to facilitate the miniaturization and weight reduction of high voltage converters for many other applications.

REFERENCES

[1] Y. He, M. Woolston, and D. Perreault, "Design and implementation of a lightweight high-voltage power converter for electro-aerodynamic propulsion," in *2017 IEEE 18th Workshop on Control and Modeling for Power Electronics (COMPEL)*, July 2017, pp. 1–9.

[2] C. K. Gilmore and S. R. H. Barrett, "Electrohydrodynamic thrust density using positive corona-induced ionic winds for in-atmosphere propulsion," *Proceedings of the Royal Society of London A: Mathematical, Physical and Engineering Sciences*, vol. 471, no. 2175, 2015.

[3] C. Gilmore, "Electro-aerodynamic thrust for fixed-wing aircraft propulsion," Ph.D. dissertation, Massachusetts Institute of Technology, 2017.

[4] H. Xu, N. Gomez-Vega, D. R. Agrawal, and S. R. H. Barrett, "Higher thrust-to-power with large electrode gap spacing electroaerodynamic devices for aircraft propulsion," *Journal of Physics D: Applied Physics*, vol. 53, no. 2, p. 025202, oct 2019. [Online]. Available: https://doi.org/10.1088%2F1361-6463%2Fab4a4c

[5] H. Akiyama, T. Sakugawa, T. Namihira, K. Takaki, Y. Minamitani, and N. Shimomura, "Industrial applications of pulsed power technology," *IEEE Transactions on Dielectrics and Electrical Insulation*, vol. 14, no. 5, pp. 1051–1064, October 2007.

[6] S. Ahn, H. Ryoo, J. Gong, and S. Jang, "Low-ripple and high-precision high-voltage dc power supply for pulsed power applications," *IEEE Transactions on Plasma Science*, vol. 42, no. 10, Oct 2014.

[7] H. Sheng, W. Shen, H. Wang, D. Fu, Y. Pei, X. Yang, F. Wang, D. Boroyevich, F. C. Lee, and C. W. Tipton, "Design and implementation of a high power density three-level parallel resonant converter for capacitor charging pulsed-power supply," *IEEE Transactions on Plasma Science*, vol. 39, no. 4, pp. 1131–1140, April 2011.

[8] A. S. Gilmour, "Power conditioning systems for high-power, airborne, pulsed applications," *IEEE Transactions on Aerospace and Electronic Systems*, vol. AES-13, no. 6, pp. 660–678, Nov 1977.

[9] I. T. Myers, E. D. Baumann, R. Kraus, and A. N. Hammound, "Multi-megawatt inverter/converter technology for space power applications," *AIP Conference Proceedings*, vol. 246, no. 1, pp. 401–409, 1992. [Online]. Available: https://aip.scitation.org/doi/abs/10.1063/1.41800

[10] L. B. Gordon, "Engineering high voltage in the space vacuum," in *Proceedings of 17th International Symposium on Discharges and Electrical Insulation in Vacuum*, vol. 2, July 1996.

[11] L. Gordon, "Power conditioning techniques," in *Neutral Particle Beam Technology Symposium*, July 1989.

[12] A. S. Gilmour, "High-power, light-weight power conditioning," *IEEE Aerospace and Electronic Systems Magazine*, vol. 6, no. 12, Dec 1991.

[13] G. E. Schwarze, "Development of high frequency low weight power magnetics for aerospace power systems," in *19th Intersoc. Energy Conversion Eng. Conf.*, August 1984.

[14] J. J. Bliss, "Some typical circuits for industrial x-ray apparatus," *Journal of the British Institution of Radio Engineers*, vol. 15, no. 2, Feb 1955.

[15] J. Sun, "Series resonant zcs–pfm dc–dc converter with multistage rectified voltage multiplier and dual-mode pfm control scheme for medical-use high-voltage x-ray power generator," *IEE Proceedings - Electric Power Applications*, vol. 147, pp. 527–534(7), November 2000.

[16] J. A. Martin-Ramos, A. M. Pernia, J. Diaz, F. Nuno, and J. A. Martinez, "Power supply for a high-voltage application," *IEEE Transactions on Power Electronics*, vol. 23, no. 4, pp. 1608–1619, July 2008.

[17] S. Iqbal, G. K. Singh, and R. Besar, "A dual-mode input voltage modulation control scheme for voltage multiplier based x-ray power supply," *IEEE Transactions on Power Electronics*, vol. 23, no. 2, pp. 1003–1008, March 2008.

[18] S. Park, L. Gu, and J. Rivas-Davila, "A compact 45 v-to-54 kv modular dc-dc converter," in *2019 20th Workshop on Control and Modeling for Power Electronics (COMPEL)*, June 2019.

[19] S. Mao, "A high frequency high voltage power supply," in *Proceedings of the 2011 14th European Conference on Power Electronics and Applications*, Aug 2011.

[20] T. B. Soeiro, J. Mühlethaler, J. Linnér, P. Ranstad, and J. W. Kolar, "Automated design of a high-power high-frequency lcc resonant converter for electrostatic precipitators," *IEEE Transactions on Industrial Electronics*, vol. 60, no. 11, pp. 4805–4819, Nov 2013.

[21] N. Grass, W. Hartmann, and M. Klockner, "Application of different types of high-voltage supplies on industrial electrostatic precipitators," *IEEE Transactions on Industry Applications*, vol. 40, no. 6, Nov 2004.

[22] S. Jang, H. Ryoo, S. Ahn, J. Kim, and G. H. Rim, "Development and optimization of high-voltage power supply system for industrial magnetron," *IEEE Transactions on Industrial Electronics*, vol. 59, no. 3, pp. 1453–1461, March 2012.

[23] I. Barbi and R. Gules, "Isolated dc-dc converters with high-output voltage for twta telecommunication satellite applications," *IEEE Transactions on Power Electronics*, vol. 18, no. 4, July 2003.

[24] C. R. Smith, "Power module technology for the 21st century," in *Proceedings of the IEEE 1995 National Aerospace and Electronics Conference. NAECON 1995*, vol. 1, May 1995.

[25] P. Bresesti, W. L. Kling, R. L. Hendriks, and R. Vailati, "Hvdc connection of offshore wind farms to the transmission system," *IEEE Transactions on Energy Conversion*, vol. 22, no. 1, pp. 37–43, March 2007.

[26] M. Stieneker, B. J. Mortimer, N. R. Averous, H. Stagge, and R. W. De Doncker, "Optimum design of medium-voltage dc collector grids depending on the offshore-wind-park power," in *2014 IEEE Symposium on Power Electronics and Machines for Wind and Water Applications*, July 2014, pp. 1–8.

[27] G. Gant, L. Jan, and R. Bartlett, "Power conditioning requirements for ion thruster systems," in *1970 IEEE Power Electronics Specialists Conference*, April 1970.

[28] H. I, "Description of a 2.3 kw power transformer for space applications," in *Aerospace High Voltage Workshop*, February 1979.

[29] J. DAVIS, E. JAMES, and P. RAMIREZ, *An advanced contact ion microthruster system*. [Online]. Available: https://arc.aiaa.org/doi/abs/10.2514/6.1968-552

[30] C. COLLETT and C. DULGEROFF, *Cesium microthruster system*. [Online]. Available: https://arc.aiaa.org/doi/abs/10.2514/6.1969-292

[31] F. C. Schwarz, "A 10 kw lightweight dc converter," in *Technical report of Power Electronics Association Inc.*, 1977.

[32] D. Fu, F. C. Lee, Y. Qiu, and F. Wang, "A novel high-power-density three-level lcc resonant converter with constant-power-factor-control for charging applications," *IEEE Transactions on Power Electronics*, vol. 23, no. 5, pp. 2411–2420, Sept 2008.

[33] N. Shafiei, M. Pahlevaninezhad, H. Farzanehfard, A. Bakhshai, and P. Jain, "Analysis of a fifth-order resonant converter for high-voltage dc power supplies," *IEEE Transactions on Power Electronics*, vol. 28, no. 1, pp. 85–100, Jan 2013.

[34] S. Park, L. Gu, and J. Rivas-Davila, "60 v-to-35 kv input-parallel output-series dc-dc converter using multi-level class-de rectifiers," in *2018 IEEE Applied Power Electronics Conference and Exposition*, March 2018.

[35] S. Mao, C. Li, W. Li, J. Popović, S. Schröder, and J. A. Ferreira, "Unified equivalent steady-state circuit model and comprehensive design of the lcc resonant converter for hv generation architectures," *IEEE Transactions on Power Electronics*, vol. 33, no. 9, Sep. 2018.

[36] Y. He, "Towards lightweight high-voltage power conversion," Ph.D. dissertation, Massachusetts Institute of Technology, 2020.

[37] W. C. Hsu, J. F. Chen, Y. P. Hsieh, and Y. M. Wu, "Design and steady-state analysis of parallel resonant dc-dc converter for high-voltage power generator," *IEEE Transactions on Power Electronics*, Feb 2017.

[38] K. Masuyama and S. R. H. Barrett, "On the performance of electrohydrodynamic propulsion," *Proceedings of the Royal Society A: Mathematical, Physical and Engineering Sciences*, Apr 2013.

[39] E. Moreau, N. Benard, J.-D. Lan-Sun-Luk, and J.-P. Chabriat, "Electrohydrodynamic force produced by a wire-to-cylinder dc corona discharge in air at atmospheric pressure," *Journal of Physics D: Applied Physics*, vol. 46, no. 47, p. 475204, oct 2013.

[40] H. Xu, Y. He, and S. R. H. Barrett, "A dielectric barrier discharge ion source increases thrust and efficiency of electroaerodynamic propulsion," *Applied Physics Letters*, vol. 114, no. 25, p. 254105, 2019. [Online]. Available: https://doi.org/10.1063/1.5100524

[41] N. Gomez-Vega, H. Xu, J. M. Abel, and S. R. H. Barrett, "Performance of decoupled electroaerodynamic thrusters," *Applied Physics Letters*, vol. 118, no. 7, 2021.

[42] H. Xu, Y. He, K. L. Strobel, C. K. Gilmore, S. P. Kelley, C. C. Hennick, T. Sebastian, M. R. Woolston, D. J. Perreault, and S. R. H. Barrett, "Flight of an aeroplane with solid-state propulsion," *Nature*, vol. 563, no. 7732, pp. 532–535, 2018.

[43] L. Raymond, W. Liang, L. Gu, and J. R. Davila, "13.56 mhz high voltage multi-level resonant dc-dc converter," in *2015 IEEE 16th Workshop on Control and Modeling for Power Electronics (COMPEL)*, July 2015.

[44] Y. He and D. J. Perreault, "Diode evaluation and series diode balancing for high-voltage high-frequency power converters," *IEEE Transactions on Power Electronics*, pp. 1–1, 2019.

[45] M. D. Seeman and S. R. Sanders, "Analysis and optimization of switched-capacitor dc–dc converters," *IEEE Transactions on Power Electronics*, vol. 23, no. 2, March 2008.
[46] G. J. Rohwein, "High-voltage air-core pulse transformers."
[47] M. Tilbury. (2008) The ultimate tesla coil design and construction guide. [Online]. Available: https://isidore.co/calibre/get/pdf/5452
[48] A. Vázquez Carazo, "50 years of piezoelectric transformers. trends in the technology," *MRS Proceedings*, vol. 785, p. D1.7, 2003.
[49] E. L. Horsley, M. P. Foster, and D. A. Stone, "State-of-the-art piezoelectric transformer technology," in *2007 European Conference on Power Electronics and Applications*, Sept 2007, pp. 1–10.
[50] S. Inc. (2019) Steminc smmtf53p2s40. [Online]. Available: https://www.steminc.com/PZT/en/multi-layer-piezo-transformer-53-khz-3w
[51] T. Inc. (2019) Transoner laminated pt. [Online]. Available: http://www.transoner.com/application-specific-data/
[52] R. L. Steigerwald, "A comparison of half-bridge resonant converter topologies," *IEEE Transactions on Power Electronics*, April 1988.
[53] V. Garcia, M. Rico, J. Sebastian, and M. M. Hernando, "Using the hybrid series-parallel resonant converter with capacitive output filter and with pwm phase-shifted control for high-voltage applications," in *Proceedings of IECON'94 - 20th Annual Conference of IEEE Industrial Electronics*, vol. 3, Sep. 1994.
[54] L. Dalessandro, F. da Silveira Cavalcante, and J. W. Kolar, "Self-capacitance of high-voltage transformers," *IEEE Transactions on Power Electronics*, vol. 22, no. 5, Sep. 2007.
[55] L. C. Raymond, W. Liang, and J. M. Rivas, "Performance evaluation of diodes in 27.12 mhz class-d resonant rectifiers under high voltage and high slew rate conditions," in *2014 IEEE 15th Workshop on Control and Modeling for Power Electronics (COMPEL)*, June 2014.
[56] W. . Gu and R. Liu, "A study of volume and weight vs. frequency for high-frequency transformers," in *Proceedings of IEEE Power Electronics Specialist Conference - PESC '93*, June 1993, pp. 1123–1129.